Structural, Optical and Dielectric Properties of $PbTi_{0.99}Zr_{0.01}TiO_3$

Kapil Vaishnave[1], Rajesh Kumar Katare[2]
[1]*Research Scholar, Dept. Of Physics, SAGE University, Indore (M.P.)-India*
[2]*Professor, Dept. Of Physics, SAGE University, Indore (M.P.)-India*

***Abstract*—$PbZr_{0.99}Ti_{0.01}O_3$, a perovskite (ABO_3), has been effectively synthesized using the ceramic synthesis method. To verify the structure of the sample , X-ray diffraction was performed on it. The single phased crystalline tertragonal structure with assigned space group P/4mmm was validated by XRD data analysis. The determined particle size, using the classical Scherer formula, was around 80 nm. The higher sintering temperature is believed to be the cause of the higher particle size. The optical bandgap of the $PbZr_{0.99}Ti_{0.01}O_3$ perovskite sample has been measured and is predicted to be 3.38 eV. After conducting dielectric experiments, it was discovered that the sample exhibited notable dielectric behavior. It is observed that the loss tangent values are modest and the electric permitivity values are comparatively superior. The electric permitivity values are relatively better and the loss tangent values are witnessed to be small. Furthermore, Electrical impedance and electrical modulus were examined to explore conduction mechanism in the as synthesized sample.**

***Index Terms*—Crystal structure, Solid state route, dielectric properties, Optical bandgap, Conduction mechanism.**

I. INTRODUCTION

All ABO_3-type materials have been the subject of extensive research. One of the ferroelectric materials that has been studied the most is lead zirconate titanate (PZT) powders, which have attracted special attention. A solid solution of lead zirconate and lead titanate, $Pb(Zr,Ti)O_3$ is of significant importance from both a basic science and a technological standpoint. Solid solutions of lead titanate zirconate ($Pb(Zr,Ti)O_3$), or PZT, crystallize into a variety of deformed perovskite forms. Because of their intriguing ferroelectric, piezoelectric, and other electrical properties, these materials have attracted a lot of attention from material scientists. Such piezoelectric materials are often used in ultrasonic generators, hydrophones, electrozero buzzers and ringers, pressure and stress sensors, etc [1-4].

One of the most crucial electric ceramic materials is ferroelectric lead zirconate titanate $Pb(Zr,Ti)O_3$, which is used in pyroelectric infrared detectors, piezoelectric transducers, ferroelectric RAM (FeRAM) gate materials, capacitors of dynamic random access memories (DRAMs), and non-linear optical devices. PZT ceramics have been extensively studied due to their promise for low temperature processing and the variety of electrical properties that may be achieved by altering the composition ratio or adding dopants. These ceramics have a high dielectric constant and a high spontaneous polarization. Since the size of devices that employ PZT will be decreasing, it is necessary to consider tuning the physical properties of PZT by managing the size of materials. Reports on nanocrystalline PZT materials are few. There are two components to the size effect: intrinsic and extrinsic. In-depth research on crystal structure and physical characteristics for both bulk and nanocrystalline materials is necessary to address the impact of size on intrinsic and extrinsic attributes of PZT materials. The synthesis technique used and the processing parameters have a significant impact on the crystallite's size [4-8].

In this context, various method of preparation have been employed. Among these preparation techniques, solid state route (SSR) is a reliable one. It esures preparation of single phase material. The problem is higher energy and time consumption. Also, the average size of crystallites is relatively large compared to other chemical processes. This project is to seek the effect of Zr, minimal doping on the pristine $PbTiO_3$ so that without any alteration in the crystal structure, the sole effect of dopant is explored. To fulfil the requisites of the objective, we explored the sample for structural, electrical and optical properties . To further explore the sample, we tried to emphasize on the conduction mechanism in the sample employing impedance and electric modulus studies. All the characterizations were

carries out at room temperature and the electric properties were measured as a response to the ac field.

II. EXPERIMENTAL DETAILS

Sample Synthesis: A polycrystalline $PbZr_{0.99}Ti_{0.01}O_3$ sample was made using the traditional solid-state reaction ceramic synthesis method. The initial materials of analytic grade were TiO_2, ZrO_2, and PbO. To create the $PbZr_{0.99}Ti_{0.01}O_3$ sample, all of these precursors were combined in stoichiometric proportions in oxide powder form. Using a pestle and agate mortar, the mixture was mechanically mashed for five hours. Acetone was employed to ensure that the sample's contents were evenly distributed. calcined for five hours at 1050 °C in air. With a calcination temperature of 1150 °C, the identical procedure was carried out again. To create a fine powder suitable for characterizations, the finished calcined material was crushed for one hour. A little portion of the fine powder so obtained was pressed into pellet form of the diameter of 10 mm and thickness nearly 1mm.under a pressure of 4 tons per inch. The circular disc shaped pellet was sintered in air at 1200 °C for 8h each. The compact form of the pellet was polished on its circular faces for electrode formation to carry out electrical measurements effectively. etc.

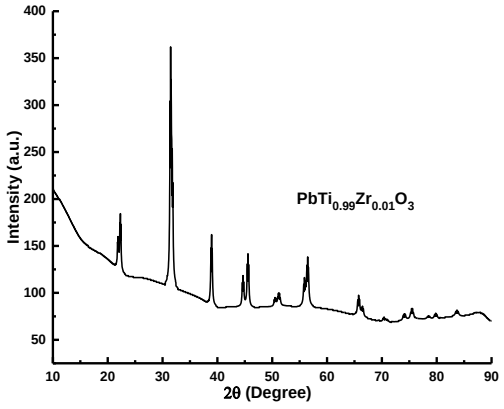

Figure 1: XRD pattern of $PbZr_{0.99}Ti_{0.01}O_3$ perovskite material

Characterizations:X-ray powder diffraction technique at room temperature is used to identify the crystal structure, type of phase and crystallite size of $PbZr_{0.99}Ti_{0.01}O_3$ sample by means Bruker D8-Advance X-ray diffractometer with Cu$K\alpha_1$ (1.5406 Å) radiation. The data was collected with a step size of 0.02° over the angular range 2θ (20° < 2θ < 80°) generating X-ray by 40 kV and 40 mA power settings. Rietveld refinement was done on the XRD data using FullProf refinement software.The sample was subjected to optical bandgap studies using UV-Vis Diffuse Reflectance Spectroscopy (DRS) employing UV–Vis spectrometer (Perkin Elmer, Lambda 950 - USA). Dielectric measurements were performed as a function of frequency in the range of 1 Hz–10MHz on Novocontrol alpha-A high performance frequency analyzer at room temperature.

III. RESULTS AND DISCUSSIONS.

STRUCTURAL ANALYSIS

The as prepared polycrystalline $PbZr_{0.99}Ti_{0.01}O_3$ sample has been structurally characterized by X-ray powder diffraction (XRD). XRD was used to determine the phase structure and purity of the as-synthesized samples. Room temperature XRD pattern of $PbZr_{0.99}Ti_{0.01}O_3$ sample is shown in Figure 1. Analysis of the XRD pattern revealed the tetragonal structure of the sample with the assigned space group *P/4mmm* [9,10]. From the appearance of the XRD patterns, no new phase is expected as revealed from the analysis. Thus purity and single phase nature is evident due to absence of any extra peak within the experimental limit. This is because the ionic radii of the B-sight Ti^{4+} (0.68Å) and Zr^{4+} (0.79Å) of ABO_3 are comparable and their inter-diffusion has been facilitated by high temperature treatment resulting in the formation of a single phased material. The narrowness of characteristic XRD peaks is due the large average crystallite size effect and the sharpness of the same peak is attributed to the high crystallinity of samples.

The average particle size (*D*) of the samples is calculated by classical Debye-Scherrer's formula:

$$d = 0.9\lambda/\beta\cos\theta$$

where, λ is the wavelength of Cu$K\alpha_1$ radiation used and β is the full width half maximum (FWHM) of the highest intense peak of diffracting angle 2θ. The average calculated particle size was about 80 *nm*.

DIELECTRIC MEASUREMENTS

Studies have been carried out on relative permitivity of $PbZr_{0.99}Ti_{0.01}O_3$ sample. The experiment was carried out at ambient conditions. The range of applied ac field is 100Hz-1MHz. The real part (ε') of dielectric constant is the measure of the amount of energy stored in a dielectric due to the applied field and is calculated by using formula $\varepsilon = ct/A\varepsilon_0$ where ε_0 is the permittivity of free space, '*t*' is the

thickness of pellet, 'A' is the cross sectional area and '*C'* is the capacitance of pellet. Figure 2 illustrates how ε' changes with frequency. Figure 2 makes it clear that for the prepared sample, the dielectric constant (ε') drops as frequency (f) increases and becomes constant at higher frequencies [10-13]. This fluctuation of ε' with f is consistent with Koop's phenomenological theory and illustrates the dispersion caused by interfacial polarization of the Maxwell-Wagner type [14,15]. The interfacial dislocations, oxygen vacancies, charged defects, grain boundaries effect, and interfacial/space charge polarization brought on by the heterogeneous dielectric structure could all be responsible for the high dielectric constant values at low frequencies.

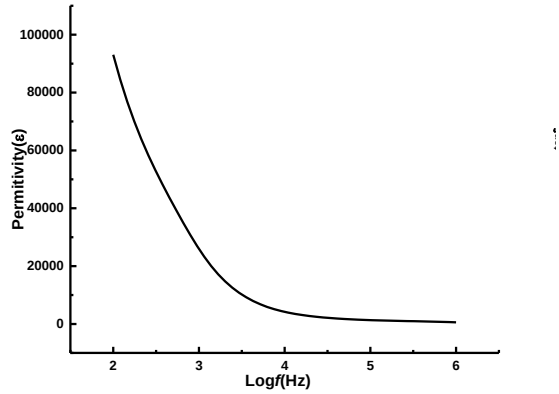

Figre 2: Dielctric constant of $PbZr_{0.99}Ti_{0.01}O_3$ sample

Figure 3 displays the fluctuation of loss tangent with frequency at room temperature. The inhibition of domain wall motion results in a decrease in dielectric loss at high frequencies. At lower frequencies, the dielectric loss is observed to be greatest. This happens when the frequency of the applied field approaches that of the electrons hopping between various ionic sites. The presence of impurities and structural inhomogeneities causes the polarization to lag behind the applied alternating field, which results in dielectric loss. At low frequencies, the dielectric loss tangent value is considerable; at higher frequencies, it gradually decreases and reaches a constant value. The dielectric loss in this investigation reaches its highest value at a specific frequency. This characteristic is attributed to the resonance between the applied electric field and the polaron hopping frequency [13-16].

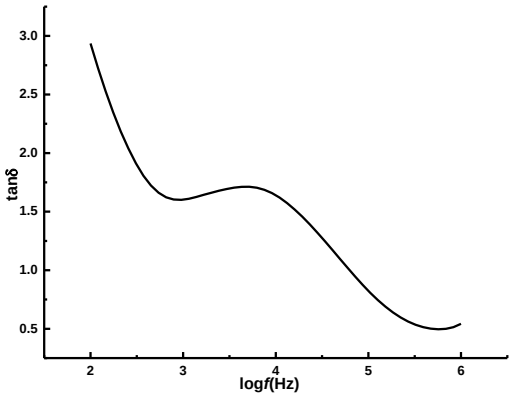

Figure 3: Dielectric loss (tanδ) of $PbZr_{0.99}Ti_{0.01}O_3$ sample

CONDUCTIVITY(σ_{ac})

The reaction is shown in Figure 4 after the conductivity behavior of the synthesized $PbZr_{0.99}Ti_{0.01}O_3$ sample was observed. According to the figure, the sample's initial ac conductivity was extremely low, and the dc conductivity was responsible for the conductivity's domination. However, the conductivity begins to increase suddenly after a certain limit in the applied field. The behavior is explained by the fact that the increase in ac conductivity is caused by the release of charges from the trap centers and defects after a threshold frequency.

ELECTRICAL IMPEDANCE

In corrosion research, semiconductor science, energy conversion and storage technologies, chemical sensing and bio-sensing, noninvasive diagnostics, and other fields, electrochemical impedance spectroscopy (EIS) provides kinetic and mechanistic data on a variety of electrochemical systems. EIS is based on applying a sinusoidal signal (ac voltage or ac current) across a broad frequency range to perturb an electrochemical system in equilibrium or steady state, and then monitoring the system's sinusoidal response (current or voltage, respectively) to the applied perturbation [10,17].

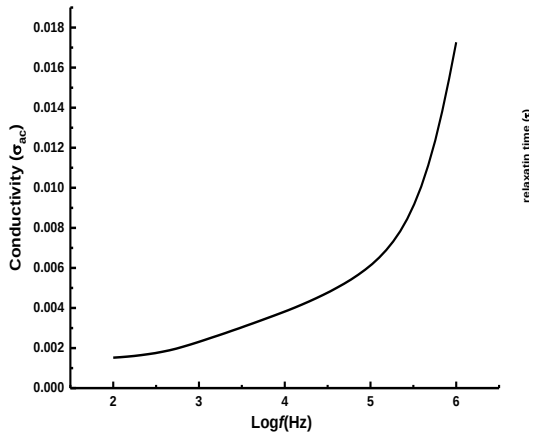

Figure 4: Conductivity (σ_{ac}) of $PbZr_{0.99}Ti_{0.01}O_3$ sample

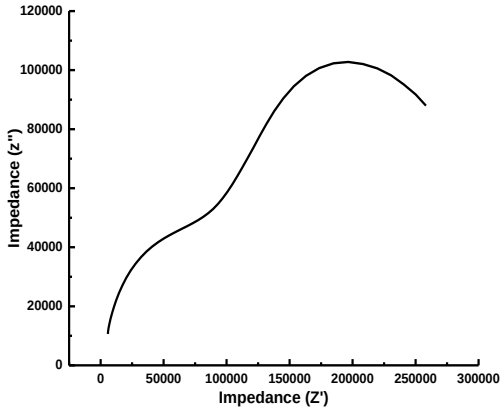

Figure 5: Impedance ((Cole-Cole Plot) of $PbZr_{0.99}Ti_{0.01}O_3$ sample

For a Faradaic impedance spectrum over a broad frequency range, the Nyquist plot pattern typically includes both the semicircle (where charge transfer phenomena control the electrochemical process) and the straight line (where mass transfer phenomena control the electrochemical process, which can vary based on the corresponding values of of *C*dl, *R*ct, and *Z*W. Three semicircles typically make up Nyquist plots: the leftmost one, which occurs at high frequencies and represents the redox charge transfer at the interface between the electrolyte and platinum counter electrode; the middle one, which occurs at intermediate frequencies and represents recombination at the electrode/electrolyte interface, from which recombination resistance can be read through the diameter; and the ion diffusion in the electrolyte, which occurs at low frequencies[10,18].

The mid-frequency peak and the rightmost one frequently coincide in EIS spectra. Recombination resistance (Rct), which is almost equivalent to the second semicircle's diameter, can be obtained using EIS. From Figure 5, almost two semicircles were seen. As can be observed, the recombination was depressed since the second semicircle's diameter of the Nyquist's plot is significantly greater [18.19]

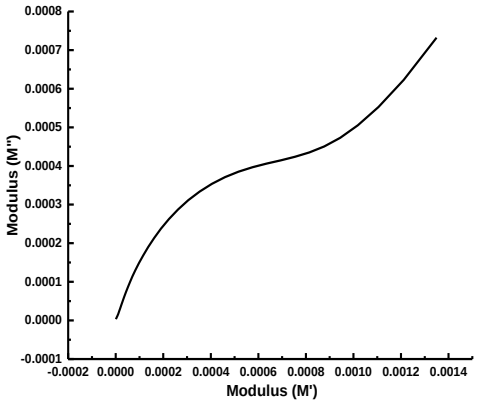

Figure 6: Electric Modulus (Nyquist's Plot) of $PbZr_{0.99}Ti_{0.01}O_3$ sample.

IV. ELECTRICAL MODULUS

Relaxation times in the conductivity phenomena can be ascertained by using the sample's electric modulus to extract the response of the sample to the applied electric field. The Cole–Cole diagrams of complex modulus plots (M″ vs. M′) for $PbZr_{0.99}Ti_{0.01}O_3$ ceramic is shown in Figure 7. The presence of tiny, asymmetric, and depressed semi-circular arcs reveals a non-Debye-type dielectric relaxation [20,21].

OPTICAL BANDGAP

The estimation of the band gap is a crucial characterization of a material for use in advanced electronic devices. The Diffuse Reflectance Spectroscope (DRS) is a straightforward and effective spectroscopic tool for estimating the bandgap of $PbZr_{0.99}Ti_{0.01}O_3$ Oxide material. The DRS spectrum was converted using the Kubelka-Munk function after measuring the UV-visible absorption spectrum of $PbZr_{0.99}Ti_{0.01}O_3$ perovskite. Plotting the square of the Kubelka-Munk-function $[F(R)hv]^2$ against energy, where R denotes reflectance, allowed for the determination of the optical band gap energy (Figure 7). Plotting $[hF(R)]^n$ against h for n = 2 produced the best fit for the plot. The energy axis is intercepted at a location by an extrapolated straight line along the curve's sharp edge, providing an estimate of the band gap. In this instance, the optical energy gap is 3.38 eV [22-24].

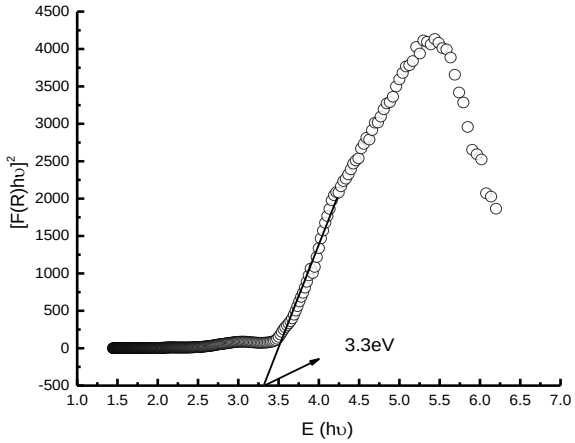

Figure 7: Optical Bandgap (Tauc'S Plot) Of $Pbzr_{0.99}Ti_{0.01}O_3$ Sample

III. CONCLUSION

We have successfully prepared a single phased and pure material of $PbZr_{0.99}Ti_{0.01}O_3$ sample using ceramic route i.e. solid state reaction method. XRD analysis confirmed the tetragonal structure of the $PbZr_{0.99}Ti_{0.01}O_3$ compound with space group *P/4mmm*. Dielectric measurements reveal that the sample exhibits an admirable dielectric constant which reduces with the increase in the frequency. The same behaviour is observed for dielectric loss where at low frequency, the loss is high which decreases with increase in the frequency. The conduction mechanism was explained in terms of Nyquist's plot and analysis of Cole-Cole plot. The optical bandgap determined was found to be 3.8eV.

ACKNOWLEDGEMENT

The authors acknowledge SAGE University, Department of physics, lab Bearers and assistants along with my researchmates without support of whom, it would have been a tough job to execute this research piece of work.

REFERENCES

[1] E. G. Popescu, M. A. Husanu, P. C. Constantinou etc. Experimental Band Structure of $Pb(Zr,Ti)O_3$: Mechanism of Ferroelectric Stabilization, dv. Sci. 10 (2023) 2205476

[2] A. Perez-Tomas,H. Xie, Z. Wan et.al., $PbZrTiO_3$ ferroelectric oxide as an electron extraction material for stable halide perovskite solar cells,Sustainable Energy Fuels, 3 (2019) 382

[3] Y. Takada, K. Mimura, K. Kato, Fabrication and piezoelectric properties of $Pb(Zr,Ti)O_3$ cubes synthesized by hydrothermal method, Journal of the Ceramic Society of Japan 126(5) (2018)326-330

[4] J. Lee, L. Johnson, A. Safari, R. Ramesh, T. Sands, H. Gilchrist, and V. G. Keramidas, "Effects of crystalline quality and electrode material on fatigue in $Pb(Zr,Ti)O_3$ thin film capacitors," Appl. Phys. Lett. vol. 63 (1993) 27-29,

[5] Sato, H., Toda, K. An application of Pb(Zr, $Ti)O_3$ Ceramic to opto-electronic devices. *Appl. Phys.* 13 (1977) 25–28

[6] T. Morikawa,M.Kodera, T. Shimizu, Domain structures of $PbTiO_3$ and $Pb(Zr,Ti)O_3$ thin films controlled by tensile strain induced by a $Sr(Zr,Ti)O_3$ buffer layer *Appl. Phys. Lett.* 124 (2024) 032901

[7] P. E.Janolin, Strain on ferroelectric thin films: Example of $Pb(Zr_{1-}xTix)O_3$, *J. Mater. Sci*, 44(19) (2009) 5025–5048

[8] V. G. Kukhar, N. A. Pertsev, H.Kohlstedt , and R. Waser , " Polarization states of polydomain epitaxial Pb $(Zr_{1-x}Ti_x)O_3$ thin films and their dielectric properties," *Phys. Rev. B* 73 (21) (2006) 214103

[9] N. Sahu, S. Panigrahi, M. Kar,Structural study of Zr doped $PbTiO_3$ materials by employing Rietveld method, Advanced Powder Technology 22 (2011) 689–694

[10] H. Sharma,R.K. Kotnala, J. Shahb , N.S. Negi,Surface, phase transition and impedance studies of Zr- mutated $BaTiO_3$ leadfree thin films,Results in Physics 13 (2019) 1021

[11] M. R. Soares, A.M.R. Senos, P.Q. Mantas, Phase coexistence region and dielectric properties of PZT ceramics, J. Euro. Ceram. Soc. 20 (2000) 321–334.

[12] M. A. Mohiddon, A. Kumar, K. L. Yadav, Effect of Nd doping on structural dielectric and thermodynamic properties of PZT (65/35) ceramics, Physica B 395 (2007) 1–9

[13] B. Noheda, D .E. Cox, G. Shirane, R. Guo, B. Jones, L. E. Cross, Stability of the monoclinic phase in the ferroelectric perovskite $PbZr_{1-x}Ti_xO_3$, Phys. Rev. B 63 (2001) 14103–14112

[14] K.W. Wagner, Zur Theorie der Unvollkommenen Dielektrika, Ann. Phys. 40 (1913) 817

[15] C. G. Koops, On the Dispersion of Resistivity and Dielectric Constant of Some Semiconductors at Audio frequencies, Phys. Rev. 83 (1951) 121

[16] Q. Xu, Z. Li, Dielectric and ferroelectric behaviour of Zr-doped $BaTiO_3$ perovskites Processing and Application of Ceramics 14(3) (2020) 188–194

[17] G. Barbero, L. Lelidis, Analysis of Warburg's impedance and its equivalent electric circuits, *Phys. Chem. Chem. Phys.*, ,19 (2017) 24934-24944

[18] V. Varade, G. V. Honnavar, P. Anjaneyulu, K. P. Ramesh, R. Menon Probing disorder and transport properties in polypyrrole thin-film devices by impedance and Raman spectroscopy. J Phys D: Appl Phys46 (2013) 365306

[19] B. Tiwari, T. Babu, R. N. P. Choudhary, AC Impedance and Modulus Spectroscopic Studies of $Pb(Zr_{0.35-x}Ce_xTi_{0.65})O_3$ (x= 0.00, 0.05, 0.10, 0.15), Ferroelectric CeramicsMaterials Chemistry and Physics 256 (2020) 123655

[20] R. Ranjan, R. Kumar, N. Kumar, B. Behera, R.N.P. Choudhary, Impedance and electric modulus analysis of Sm modified $Pb(Zr_{0.55}Ti_{0.45})_{1-x/4}O_3$ ceramics, J. Alloys Compd. 509 (2011) 6388–6394.

[21] B. Tiwari, R.N.P. Choudhary, Frequency-temperature response of $Pb(Zr_{0.65-x}Ce_xTi_{0.35})O_3$ ferroelectric ceramics: impedance spectroscopic studies, J. Alloys Compd. 493 (2010) 1–10

[22] P. Prajapati and A. K. Singh, Band gap tuning of ferroelectric $PbTiO_3$ by Mo doping J Mater Sci: Mater Electron 33 (2022) 2550–2565

[23] D. G. Popescu, M. A. Husanu, P. C. Constantinou, Experimental Band Structure of $Pb(Zr,Ti)O_3$: Mechanism of Ferroelectric Stabilization, Advanced Science,10(6) (2023) 2205476

[24] C. C. Parhi, A. B.Thirumalasetty, A. R. James, and M. Wuppulluri: Relative Investigation on Microwave-Assisted Zr-Modified $PbTiO_3$ and $BaTiO_3$ Ferroelectric Ceramics for Energy Storage Application ACS Omega, 8, (2023) 37752−37768